Title

Backbone Hydrocarbon-Constrained Nucleic Acids Modulate Hybridization Kinetics for RNA

Journal

Journal of the American Chemical Society, 144(4)

ISSN

0002-7863

Authors

Rajasekaran, Tamilselvan
Freestone, Graeme C
Galindo-Murillo, Rodrigo
et al.

Publication Date

2022-02-02

DOI

10.1021/jacs.1c12323

Peer reviewed

HHS Public Access

Author manuscript

J Am Chem Soc. Author manuscript; available in PMC 2022 October 02.

Published in final edited form as:

J Am Chem Soc. 2022 February 02; 144(4): 1941–1950. doi:10.1021/jacs.1c12323.

Backbone hydrocarbon-constrained nucleic acids modulate hybridization kinetics for RNA

Tamilselvan Rajasekaran[#,1], **Graeme C. Freestone**[#,2], **Rodrigo Galindo-Murillo**[#,3], **Barbara Lugato**[1], **Lorena Rico**[1], **Juan C. Salinas**[1], **Hans Gaus**[2], **Michael T. Migawa**[2], **Eric. E. Swayze**[2], **Thomas E. Cheatham III**[3], **Stephen Hanessian**[1], **Punit P. Seth**[2]

[1]Department of Chemistry, University of Montreal, Quebec H3C 3J7, Canada

[2]Department of Medicinal Chemistry, Ionis Pharmaceuticals, 2855 Gazelle Court, Carlsbad, CA 92010, USA.

[3]Department of Medicinal Chemistry, College of Pharmacy, University of Utah, 2000 East 30 South Skaggs 201, Salt Lake City, UT 84112, USA.

Abstract

The binding affinity of therapeutic oligonucleotides (ONs) for their cognate RNA is determined by the rates of association (k_a) and dissociation (k_d). Single stranded ONs are highly flexible and can adopt multiple conformations in solution some of which may not be conducive for hybridization. We investigated if restricting rotation around the sugar-phosphate backbone, by tethering two adjacent backbone phosphonate esters using hydrocarbon bridges, can modulate hybridization kinetics of the modified ONs for complementary RNA. Given the large number of possible analogs with different tether lengths and configurations at the phosphorus atoms, we employed molecular dynamic simulations to optimize the size of the hydrocarbon bridge to guide the synthetic efforts. The backbone constrained nucleotide trimers with stereo-defined configurations at the contiguous backbone phosphorus atoms were assembled using a ring closing metathesis reaction, then incorporated into oligonucleotides by an *in situ* synthesis of the phosphoramidites followed by coupling to solid-supports. Evaluation of the modified oligonucleotides revealed that 15-membered macrocyclic-constrained analogs displayed similar or slightly improved on-rates but significantly increased off-rates compared to unmodified DNA ONs resulting in reduced duplex stability. In contrast, LNA ONs with conformationally pre-organized furanose rings showed similar on-rates as DNA ONs but very slow off-rates, resulting in net improvement in duplex stability. Furthermore, the experimental data generally supported the molecular simulation results suggesting that this strategy can be used as a predictive tool for designing the next generation of constrained backbone ON analogs with improved hybridization properties.

Graphical Abstract

Address correspondence to: Thomas E. Cheatham III; tec3@utah.edu, Stephen Hanessian, stephen.hanessian@umontreal.ca, Punit P. Seth, Tel. 760-603-2587, pseth@ionisph.com.

[#]co-first authors

Supporting information – Detailed experimental protocols and ^{1}H, ^{13}C and ^{31}P NMR spectra for all synthetic intermediates; determination of absolute stereochemistry of allyl triester intermediates by correlation with products derived from Baran's auxiliaries; T_m data to confirm stereochemical assignment of intermediates **5** and **5a**; analytical data for synthesized ONs and sensorgrams for ONs 1–17 is provided.

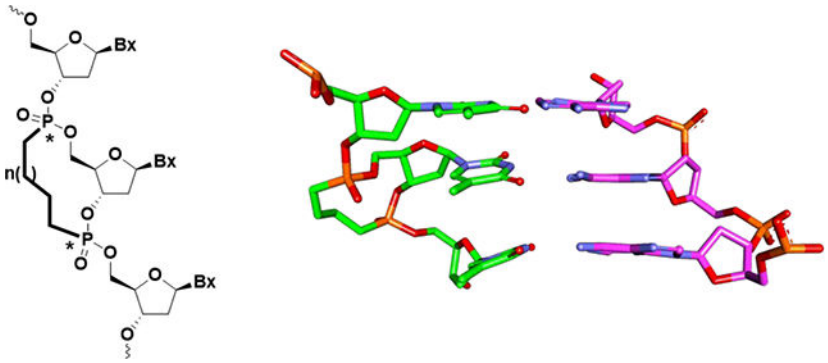

Introduction

RNA-targeting nucleic acid therapeutics have made tremendous advances in the past decade [1–2]. No less than 14 nucleic acid-based medicines have been approved by regulatory agencies and over one hundred are in early to late-stage clinical development. Improved clinical performance of antisense therapeutic drugs has, in large part, been driven by advances in delivery strategies of chemically modified oligonucleotides as drug candidates[3].

With the exception of aptamers and immunomodulatory oligonucleotides, nucleic acid-based therapeutics must hybridize with their target RNA inside cells, while avoiding interactions with mismatched RNA, to maintain the specificity of gene knockdown. The efficiency of this process is governed in part by the kinetics of association (on-rate) and dissociation (off-rate) to the targeted RNA (Figure 1A) [4]. The majority of the chemical modifications employed in nucleic acid-directed therapeutics enhance affinity for RNA by conformational restriction of the ribose-sugar [5–7]. However, the improvements in hybridization parameters using these modifications are driven primarily by reduction in off-rates once duplex-formation has been established [8]. In contrast, on-rates for modified nucleic-acids are essentially unchanged as the transition state for hybridization is established before the strands form any significant number of native base pairs [9]. Thus, chemical strategies that can modulate binding kinetics for hybridization to the targeted RNA could be useful for further improving the next generation of nucleic acid therapeutics.

We envisioned a strategy where the backbone of highly flexible single stranded oligonucleotides [10] could be constrained in a manner conducive to hybridization that would be independent of the sequence of the oligonucleotide. We hypothesized that restricting the conformational flexibility of a trinucleotide subunit by constraining the phosphate backbone using a macrocyclic hydrocarbon tether could pre-organize the nucleobases into the appropriate conformation for Watson-Crick base-pairing and modulate the kinetics of RNA-hybridization (Figure 1A). Given the large number of possible analogs with different tether lengths and configurations at the bridging phosphonates (Figure 1B), we employed molecular dynamic simulations to optimize the size of the macrocyclic hydrocarbon bridge to guide the synthetic efforts. In this report, we describe the synthesis of backbone-constrained trinucleotides incorporating tetra- and octa- methylene units to bridge

phosphonate esters linking successive 2'-deoxy thymidine units and demonstrate that their incorporation into oligonucleotides can modulate hybridization kinetics.

Experimental Section

Synthesis of phosphoramidite building blocks and modified oligonucleotides.

Complete details for the synthesis and structural characterization of the nucleoside intermediates are provided in the supporting information. The phosphoramidites were synthesized by treatment of the P-macrocyclic 2'-deoxythymidine trimers (17 mmol) with 2-cyanoethyl N,N-diisopropylchlorophosphoramidite (1.5 eq.) and DIEA (4 eq) in DCM (0.1 M) at room temperature for 2 h. Concomitantly, the DMT protecting group was removed from 15 mg of PS-200 resin in an ABI column containing the first 5 nucleobases on an ABI Synthesizer. The reaction mixtures containing the above phosphoramidites were then taken up into a 1 mL syringe and attached to one end of the ABI column. 500 μL of activator solution (1M DCI,0.1M NMI in MeCN) was taken up into a second 1 mL syringe and attached to the other end of the ABI column. The reaction mixture and activator solution were pushed back and forth through the ABI column for 15 minutes to allow for complete reaction before being discarded. The column was reattached to the ABI Synthesizer to complete the oligonucleotide synthesis using standard automated phosphoramidite chemistry.

Thermal denaturation measurements.

ASO and RNA were mixed in 1:1 ratio (4 μM duplex) in a buffer containing 100mM NaCl, 10 mM phosphate and 10 mM EDTA at pH 7. Oligos were hybridized with the complementary RNA strand by heating duplex to 85 °C for 5 min and allowed to cool at room temperature. Thermal denaturation temperatures (Tm values) were measured in quartz cuvettes (pathlength 1.0 cm) on a Cary 100 ultraviolet (UV)/visible spectrophotometer equipped with a Peltier temperature controller. Absorbance at 260 nm was measured as a function of temperature using a temperature ramp of 0.5 °C per min. Tm values were determined using the hyperchromicity method incorporated into the instrument software.

On- and off-rate measurements

Binding of oligonucleotides to complement RNA was performed on a Biacore X100 surface plasmon resonance (SPE) instrument. 100 units of complementary RNA was immobilized on a SA chip by injecting a 20 nM solution of 5'-Biotin-labeled RNA (5'-Biotin-UCGAGAAACAUCC-3') in HPS-EP buffer (10 mM HEPES, pH 7.4, 150 mM NaCl, 3 mM EDTA, 0.0005% Surfactant P20). Binding was evaluated by injecting increasing concentration of oligonucleotides (6.75nM to 100 nM, 2-fold dilution) in HPB-EP buffer at 25°C onto RNA-immobilized SA chip. Kinetic and equilibrium binding analysis was performed using Biacore X100 Evaluation Software applying 1:1 binding fit.

Results

Molecular modelling to determine optimal size of macrocyclic methylene tethers

To determine the optimal ring size and stereochemistry of the macrocyclic constrained analogs to modulate hybridization kinetics, we first evaluated analogs such as IV (Figure 2) in Molecular Dynamics simulations (MD). Using the sequence d(GGATGTTTCTCGA) and its RNA complementary chain, we built the bis-allyl phosphonate linkages (III, Figure 2) in conjunction with 11 to 15 membered tetra-and octa- methylene-bridged rings, to determine the ability of these structural modifications to form stable Watson-Crick pairing with RNA (only 11 and 15 membered rings shown).

Using DS-Visualizer 2020, we generated a double-strand B-DNA with the sequence d(GGATGTTTCTCGA). This sequence was used as a reference in further structural analysis. The cycles were created by building the different hydrocarbon bridges in DS-Visualizer and optimizing the structure using DFT with the M06/6–31G* level of theory and basis. Hydrogen atoms of the terminal carbons of the linker were deleted and a bond between the carbons and the phosphorous group of the corresponding thymine base was added using the tleap module of AmberTools [11–12]. Charges of the hydrocarbon bridge was calculated with the G09 version of the Gaussian program with HF/6–31G* and fitted using the restrained electrostatic potential module(RESP)[13] in Ambertools; bonds, angles, dihedral and improper terms were described by the General Amber Force Field [14]. The final charge of the complete cycle was manually adjusted to reach a neutral charge. DNA was described by the OL15 force field [15–16] and RNA was described by the OL3 force field [17–18]. Sodium ions where added to all the models to neutralize charge and an excess of NaCl ions using the Joung-Cheatham parameters [19] were also incorporated in order to reach a final concentration of ~200mM. The systems were solvated in a truncated octahedral periodic box with a buffer between the distance of the solute and the edge of the box of 12 Å. The optimum point charge water model (OPC)[20] was used for all the simulations.

The generated topology and coordinate files were energy minimized and equilibrated in a 10-step process. The initial step involved a 10 kcal/mol·Å^2 restraint in all the solute atoms using a 1 fs time step, allowing the solvent to relax for 1 ns; after this step, nine consecutive equilibration simulations were run for 1 ns gradually lowering the restraint constant in the solute until no restraint was present. The last step was an NTP simulation for 10 ns with no restraints. Production molecular dynamics runs were calculated for 5 μs for all the systems. Periodic boundary conditions were used, the temperature was 300K using Langevin dynamics [21] with a collision frequency of 1.0, pressure regulation was performed using the Berendsen barostat [22] and bonds containing hydrogen atoms where constrained using the SHAKE algorithm [23]. Production simulations were run using the Hydrogen Mass repartition scheme [24] allowing for a 4 fs time step. Each MD simulation was sampled for 5 μs.

Visual inspection of the trajectories revealed that the three systems indeed produced stable, although distorted duplexes for the entire simulation. The representative structure of the most populated cluster for each system is presented in Figure 3. The normalized root means square deviation (RMS) population for the test sequence (black) with no modification to the phosphodiester linkage is presented in each of the studied stereo isomers as a control.

The control DNA simulation shows deviation values between ~1–2.5 Å as observed with previous simulations with this force field [15].

The 11 ring systems shows RMS deviation from ~3–10 Å for the *R,R, S,R* and *S,S* stereochemistry and reduced structural deviation for the *R,S* configuration (Figure 3, top row). The *R,R* and *R,S* configurations show that the bis-allyl and the r15 systems are closer in value with each other, and to the control simulation. The RMS data of the r15 system with the *S,R* and *S,S* configurations suggest a lower structural deformation than the bis-allyl modification. Overall, all three systems produced duplexes regardless of the backbone stereochemistry but the 15-membered macrocyclic analogs appeared to be structurally closer to the DNA control relative to the 11-membered analogs. To determine if the results from the molecular dynamics simulation could be used as a tool to guide the synthesis effort, we undertook synthesis of all four P-diastereomers of the 11- and 15-membered 2'-deoxythymidine trimer building blocks, incorporated them into oligonucleotides and measured their duplex stabilizing properties and their ability to modulate hybridization kinetics.

Design and retro-synthesis of macrocyclic phosphonate hydrocarbon- bridged oligonucleotides

The emergence of the Grubbs ring closing metathesis reaction as a powerful method to introduce ring constructs of varying sizes starting with olefinic substrates [25], allowed Nielsen and coworkers to first explore the introduction of backbone constrained carbon-bridged phosphate esters in oligonucleotides [26]. Indeed, a variety of analogues were synthesized varying in their positions of phosphate ester attachment between dinucleotide units and the size of the olefinic carbon bridge intended to provide conformational constraint [27–29]. Given that such phosphate esters are chemically unstable to basic conditions used during deprotection of oligonucleotides after synthesis, and their dependence on inherent stereoelectronic effects that dictate the spatial orientation of the P-O bonds, we chose to use *phosphonate esters as tetra- and octa- methylene-bridged macrocycles* that link two adjacent dinucleotide units encompassed within a 2'-deoxythymidine trimer (Figure 1B). We were also cognizant from recent reports, that these linkages can result in dramatic improvements in therapeutic index for certain classes of therapeutic oligonucleotides [30].

Critical to the realization of these proposals was the accessibility of diastereomeric pairs of phosphonate esters harboring stereogenically pure phosphorus atoms within each macrocyclic construct (Figure 2). We deemed it necessary to put a premium on stereochemistry at phosphorus, in case it would play a role in the proper preorganization of the nucleoside units for recognition and hybridization. Consequently, we undertook the arduous task to synthesis *all four* diastereomeric analogs with defined stereochemistry at the phosphorus atoms.

Synthesis of macrocycles with 11 and 15-membered ring systems

The synthesis of 11-and 15 –membered methylene-bridged phosphonate macrocycles are shown in Scheme 1. Coupling of 5'-O-dimethyltrityl 2'-deoxythymidine **1** with allyl phosphoramidite **2** afforded the ester **3** which was converted to the (*R*)- and (*S*)- dimers

5 and **5a** respectively which were readily separated by column chromatography (Supporting Information Figure 1). Cleavage of the DMTr group of the (*R*)-dimer **5** followed by coupling with the allyl (**3**) or heptenyl (**7**) phosphonate esters led to the trimers **8** and **9** respectively. Ring closing metathesis with the second generation Hoveyda-Grubbs catalyst[25], followed by hydrogenation of the double bond led to a pair of diastereomeric trimers designated as (*R*/*R*)-**10** (n=11) and (*S*/*R*)-**12** (n=11) respectively. The corresponding (*R*/*R*)-**11** (n=15) and (S/R)-**13** (n=15) diastereomeric pairs were similarly prepared. Cleavage of the TBS group led to **14** and **16** (n=11) and **15** and **17** (n=15) without stereochemical erosion, which were utilized in the oligonucleotide synthesis toward designated oligonucleotide constructs (see below). Starting with the (*S*)-dimer **5a** and following the same protocol afforded the **14a**/**15a** and **16a** /**17a** diastereomeric quartet.

The diastereoisomeric dimers **5** and **5a** which were the starting materials for the 11- and 15-membered macrocyclic constructs were separated in multi-gram quantities by silica gel chromatography. It is well established that the dimer with Rp stereochemistry elutes first and has a higher melting temperature when incorporated into oligonucleotides [31–33]. To confirm this, we converted dimers **5** and **5a** into the corresponding phosphoramidites and incorporated them into oligonucleotides for evaluation in thermal denaturation experiments (Supporting information Figure S2). As suggested by literature precedence, the oligonucleotide incorporating the faster eluting dimer showed higher T_m and was confirmed as the Rp stereoisomer. The stereochemistry of the second stereocenter at phosphorus in the nucleoside trimers 14–17 and 14a-17a was assigned by careful comparison of ^{1}H, ^{31}P NMR data and optical rotation values with the corresponding phosphonates of known absolute stereochemistry prepared using the Baran achiral auxiliary [33] (Supporting information Figure S3, Schemes A and B). [33]

Incorporation of macrocyclic trimers into oligonucleotides

Each of the diastereomerically pure P-macrocycles from Scheme 1 was inserted into a series of oligonucleotide (ON) constructs to furnish the corresponding modified ASO. Given the challenging synthesis and purification protocols to obtain nucleoside trimers **14**-**17** and **14a**-**17a**, we developed a method for in situ synthesis and coupling of the nucleoside phosphoramidites (Scheme 2). The trimers **14**-**17** and **14a**-**17a** were reacted with 2-cyanoethyl *N*,*N*-diisopropylchlorophosphoramidite (1.5 eq.) and diisopropylethylamine (4 eq.) in dichloromethane (0.1 M) at room temperature for two hours. The amidite formed was not purified but instead directly coupled to a 5-mer DNA oligonucleotide on solid support using a hand-coupling protocol as described in the methods section. The synthesis column with the coupled trimer was reattached to the DNA synthesizer to complete the synthesis using standard automated phosphoramidite chemistry. Deprotection and cleavage from support and purification by ion-exchange chromatography furnished the final oligonucleotides (Supplementary Figure 4).

Effect of macrocyclic tethers on duplex thermal stability versus complementary RNA

DNA ONs modified with the 11-membered macrocyclic backbone-constrained analogs derived from ring-closing metathesis of the bis-allyl trinucleotides **14**, **16** and **14a**, **16a** were evaluated in thermal denaturation experiments. To our disappointment, these analogs

resulted in significant duplex destabilization (Table 1, **ONs 6–9**). We also measured the melting temperatures of duplexes derived from all four phosphonate diastereomers of the precursor bis-allyl nucleosides **8**, **8a** and **9**, **9a** with complementary RNA (Table 1, **ONs 2–5**). Introducing allyl substitution on adjacent phosphorus atoms in the oligonucleotide backbone also resulted in significant configuration-dependent duplex destabilization, suggesting that the destabilization observed with the 11-membered macrocyclic analogs was in-part a result of replacing the charged phosphodiester linkage with a neutral alkyl phosphonate linkage. The loss of duplex stability upon introduction of neutral phosphonate linkages could be attributed to disruption of the water of hydration spine that is important for maintaining the stability of oligonucleotide duplexes [34]. Alternatively, neutralization of the backbone charge could weaken the anomeric effects that help stabilize phosphate backbone conformations required for optimal hybridization with complementary nucleic acids [35].

In contrast, evaluation of the 15-membered macrocycle modified oligonucleotides revealed that they possessed significantly improved duplex stabilization properties relative to the 11-membered macrocycles (Table 1, **ONs 10–13**). The macrocyclic analog with the *S,R* configuration at contiguous phosphorus atoms displayed the optimal hybridization properties which were similar to unmodified ON1 and significantly improved relative to the corresponding bis-allyl analog. The macrocyclic analogs with *R,S* and *S,S* phosphorus configurations were destabilizing relative to the unmodified ON1 but were significantly more stabilizing as compared to their ring opened bis-allyl counterparts. Overall, the four P-diastereomeric 15-membered macrocyclic ONs displayed better duplex stabilizing properties as compared to the smaller 11-membered macrocycles. These results were consistent with the molecular modeling data which had suggested that the 15-membered ring would be less disruptive for duplex stability.

Effect of macrocyclic tethers on hybridization kinetics versus complementary RNA

We next characterized the hybridization kinetics of the modified ONs (Table 1). On- and off-rates of **ONs 1–13** to complementary RNA were determined using plasmon surface resonance. Measurements were accomplished by monitoring hybridization of the ONs to the biotin-labeled RNA immobilized onto a streptavidin chip. On- and off-rates were determined from the sensorgrams and binding constants calculated from measured rates (Supporting information, Figure S4).

The bis-allyl modified ONs generally displayed on-rates that were comparable or slightly faster as compared to the parent **ON1**. Presumably, the reduction of overall charge resulting from introduction of two neutral linkages may reduce charge repulsion as the two polyanionic oligonucleotides approach each other to establish hybridization. However, these analogs also resulted in faster off-rates suggesting that the neutral linkages reduce stability after duplex formation. Interestingly, on- and off-rates were dependent on configuration at phosphorus suggesting a steric and/or electronic component. Unfortunately, we were unable to get reliable data for the 11-membered macrocycle modified ONs because of their poor hybridization properties. In contrast, the 15-membered macrocycle modified ONs displayed interesting hybridization kinetics. The *S,S* analog **ON11** showed a 4.5-fold enhancement in on-rate for complementary RNA but this analog also exhibited a 37-fold faster off-rate

as compared to the parent **ON1** and its ring opened bis-allyl counterpart **ON3**. In contrast, the *R,R* analog **ON13** showed similar on- and off-rates relative to its ring opened bis-allyl counterpart **ON5**, but a 1.5-fold enhancement in on-rate relative to the parent **ON1**. The S,R (**ON10**) and R,S (**ON12**) analogs displayed very similar hybridization kinetics as the parent DNA **ON1**.

To determine how the hybridization kinetics of the macrocycle constrained analogs compare to that of other conformationally restricted modifications such as LNA that provide large enhancements in duplex stability and RNA-affinity [36–37], we measured these parameters for LNA modified ONs **14**-**17**. As expected, all LNA ONs showed excellent improvements in duplex thermal stability. Interestingly, all LNA ONs including **ON17** with three LNA incorporations, showed similar on-rates as the parent DNA **ON1** but extremely slow off-rates that were difficult to measure at 25 °C. These data demonstrate that conformational restriction of the furanose sugar enhances RNA-binding affinity by slowing off-rates after duplex formation is established and have modest to no effect on on-rates.

Discussion

Hybridization of therapeutic oligonucleotides to their RNA targets inside cells is governed in part by the rates of association (on-rates) and dissociation (off-rates). Froehler et al reported the hybridization kinetics of C5-propyne and C5-thiazole-substituted pyrimidine analogs of DNA, and showed that the aromatic C-5 substituent reduced off-rates by enhancing stacking interactions [8]. Hall recently showed that polyamine substituted C5-triazole pyrimidine analogs display significant enhancements in on-rate for complementary RNA [38–39]. However, these strategies are primarily applicable for pyrimidine nucleobases which can potentially limit their application for a broad array of sequences typically encountered in nucleic acid-based drug discovery. We envisioned a strategy where the backbone of highly flexible single stranded oligonucleotides [10] could be constrained in a manner conducive to hybridization that would be independent of the sequence of the oligonucleotide. We hypothesized that restricting the conformational flexibility of a trinucleotide subunit by constraining the phosphate backbone using a macrocyclic hydrocarbon bridge between phosphonate units could pre-organize the nucleobases into the appropriate conformation for Watson-Crick base-pairing and improve on-rates for RNA-hybridization.

We first performed molecular dynamics simulation of DNA/RNA oligonucleotide duplexes where the DNA strand was modified with 11- and 15-membered macrocyclic analogs to help determine the optimal length of the bridging methylene moiety and configuration at phosphorus for optimal hybridization. This exercise suggested that the 11-membered macrocyclic analogs produce large distortions in backbone geometries relative to the 15-membered macrocyclic analogs. To test this hypothesis, we synthesized all four P-diastereoisomers of the 11 and 15-membered macrocyclic trimers, incorporated them into oligonucleotides, and measured their duplex stabilizing and hybridization kinetics versus complementary RNA.

The open-chain bis-allyl trinucleotides showed a configuration- dependent destabilization of duplex stability (−2.6 to −11.4 °C). Replacing the negatively charged phosphodiester

backbone with neutral linkages can result in reduced duplex stability by potentially destabilizing the anomeric effects that pre-organize and/or stabilize optimal phosphodiester backbone conformations in oligonucleotide duplexes [35]. Consistent with the molecular dynamics simulation data, the 11-membered macrocycle modified oligonucleotides showed a configuration dependent destabilization in duplex thermal stability relative to the unmodified oligonucleotide (−15.1 to −19.2 °C) and the bis-allyl ring opened analogs (−6.4 to −16.6 °C). Unfortunately, the poor hybridization properties precluded measurement of hybridization kinetics for the 11-membered macrocyclic analogs. In contrast, the 15-membered analogs were significantly more stabilizing relative to the 11-membered analogs and the bis-allyl controls (−4.5 to +5.6 °C) but they did not improve duplex stability relative to the unmodified DNA ON. It is likely that this destabilization is a result of neutralizing backbone charge as opposed to enforcing a conformational constraint given the destabilization observed with the bis-allyl open chain analogs. However, the 15-membered analogs displayed interesting effects on hybridization kinetics, with the *S,S* analog exhibiting a 4-fold improvement in on-rates and a 37-fold increase in off-rates versus complementary RNA relative to the unmodified oligonucleotide. In contrast, a fully charge-neutral peptide nucleic acid (PNA) only produced a modest 2-fold improvement in on-rate for complementary RNA [40].

We also measured the hybridization kinetics of ONs modified with LNA which increases affinity by conformationally restricting the furanose ring in the N-type sugar pucker. LNA ONs displayed similar on-rates as the unmodified DNA ON but extremely slow off-rates. While this hybridization profile showed tremendous improvements in overall binding affinity, slow off-rates could be detrimental for therapeutic applications and result in toxicities if ASOs bearing these modifications are trapped at off-target sites. Indeed, progress of LNA ASOs in the clinic has been stymied by toxicity issues [41–44]. Interestingly, introducing two alkyl phosphonate linkages in ASOs bearing LNA-like high affinity modifications resulted in large improvement sin therapeutic index [30]. While these ASO designs showed reduced binding to paraspeckle proteins implicated in ASO toxicities [45], changes in hybridization to cellular RNA may have also played a role in improving therapeutic index. It is conceivable that faster hybridization (both on and off) kinetics may allow a therapeutic oligonucleotide to sample the RNA sequence-space at a faster rate and potentially improve specificity by avoiding being trapped at partially matched RNA sites.

Conclusion

Overall, our data suggest that macrocyclic bridges that restrict mobility around the phosphodiester backbone in oligonucleotides can modulate duplex thermal stability and hybridization kinetics versus complementary RNA. Our data also suggest that further optimization such as changing the tethering positions to different sites on the furanose sugar, or combining these with conformationally constrained sugar moieties, could provide additional benefits. Optimization of these properties will provide the desired chemically modified nucleoside oligomers to help determine if modulating hybridization kinetics can improve the antisense properties of oligonucleotide therapeutics. Importantly, the experimental data supported the molecular simulation results suggesting that this strategy

can be used as a predictive tool for designing the next generation of constrained backbone oligonucleotide analogs with improved hybridization properties.

Supplementary Material

Refer to Web version on PubMed Central for supplementary material.

Acknowledgements –

We thank the Center for High Performance Computing at the University of Utah. SH acknowledges financial support from NSERC Canada and Ionis Pharmaceuticals. The Cheatham lab acknowledges funding from the NIH (R-01 GM-081411) and NSF (OAC-1818253) and a Leadership Resource Allocation MCB20008 for computer time on the Frontera and Longhorn resources at the Texas Advanced Supercomputer Center and also significant computational resources from the Center for High Performance Computing at the University of Utah

References

1. Crooke ST; Witztum JL; Bennett CF; Baker BF, RNA-Targeted Therapeutics. Cell Metabolism 2018, 27 (4), 714–739. [PubMed: 29617640]
2. Shen X; Corey DR, Chemistry, mechanism and clinical status of antisense oligonucleotides and duplex RNAs. Nucleic Acids Res. 2018, 46 (4), 1584–1600. [PubMed: 29240946]
3. Wan WB; Seth PP, The Medicinal Chemistry of Therapeutic Oligonucleotides. J. Med. Chem. 2016, 59 (21), 9645–9667. [PubMed: 27434100]
4. Corey DR, 48000-fold Acceleration of Hybridization by Chemically Modified Oligonucleotides. J. Am. Chem. Soc. 1995, 117 (36), 9373–9374.
5. Leumann CJ, DNA analogues: from supramolecular principles to biological properties. Bioorg. Med. Chem. 2002, 10 (4), 841–54. [PubMed: 11836090]
6. Allart B; Khan K; Rosemeyer H; Schepers G; Hendrix C; Rothenbacher K; Seela F; Aerschot AV; Herdewijn P, D-Altritol Nucleic Acids (ANA): Hybridisation Properties, Stability, and Initial Structural Analysis. Chem.-Eur. J. 1999, 5, 2424 – 2431.
7. Wengel J, Synthesis of 3'-C- and 4'-C-Branched Oligodeoxynucleotides and the Development of Locked Nucleic Acid (LNA). Acc. Chem. Res. 1999, 32 (4), 301–310.
8. Gutierrez AJ; Matteucci MD; Grant D; Matsumura S; Wagner RW; Froehler BC, Antisense gene inhibition by C-5-substituted deoxyuridine-containing oligodeoxynucleotides. Biochemistry 1997, 36 (4), 743–8. [PubMed: 9020771]
9. Whitley KD; Comstock MJ; Chemla YR, Elasticity of the transition state for oligonucleotide hybridization. Nucleic Acids Res. 2017, 45 (2), 547–555. [PubMed: 27903889]
10. Plumridge A; Meisburger SP; Pollack L, Visualizing single-stranded nucleic acids in solution. Nucleic Acids Res. 2017, 45 (9), e66. [PubMed: 28034955]
11. Pearlman DA; Case DA; Caldwell JW; Ross WS; Cheatham TE; DeBolt S; Ferguson D; Seibel G; Kollman P, AMBER, a package of computer programs for applying molecular mechanics, normal mode analysis, molecular dynamics and free energy calculations to simulate the structural and energetic properties of molecules. Comput. Phys. Commun. 1995, 91 (1), 1–41.
12. Case DA; Cheatham TE 3rd; Darden T; Gohlke H; Luo R; Merz KM Jr.; Onufriev A; Simmerling C; Wang B; Woods RJ, The Amber biomolecular simulation programs. J. Comput. Chem. 2005, 26 (16), 1668–88. [PubMed: 16200636]
13. Wang J; Cieplak P; Kollman PA, How well does a restrained electrostatic potential (RESP) model perform in calculating conformational energies of organic and biological molecules? J. Comput. Chem. 2000, 21 (12), 1049–1074.
14. Wang J; Wolf RM; Caldwell JW; Kollman PA; Case DA, Development and testing of a general amber force field. J. Comput. Chem. 2004, 25 (9), 1157–74. [PubMed: 15116359]
15. Galindo-Murillo R; Robertson JC; Zgarbová M; Šponer J; Otyepka M; Jurečka P; Cheatham TE, Assessing the Current State of Amber Force Field Modifications for DNA. Journal of Chemical Theory and Computation 2016, 12 (8), 4114–4127. [PubMed: 27300587]

16. Dans PD; Ivani I; Hospital A; Portella G; González C; Orozco M, How accurate are accurate force-fields for B-DNA? Nucleic Acids Res. 2017, 45 (7), 4217–4230. [PubMed: 28088759]
17. Beššeová I; Banáš P; Kührová P; Košinová P; Otyepka M; Šponer J, Simulations of A-RNA Duplexes. The Effect of Sequence, Solute Force Field, Water Model, and Salt Concentration. The Journal of Physical Chemistry B 2012, 116 (33), 9899–9916. [PubMed: 22809319]
18. Zgarbová M; Otyepka M; Šponer J; Mládek A; Banáš P; Cheatham TE; Jurečka P, Refinement of the Cornell et al. Nucleic Acids Force Field Based on Reference Quantum Chemical Calculations of Glycosidic Torsion Profiles. Journal of Chemical Theory and Computation 2011, 7 (9), 2886–2902. [PubMed: 21921995]
19. Joung IS; Cheatham TE, Molecular Dynamics Simulations of the Dynamic and Energetic Properties of Alkali and Halide Ions Using Water-Model-Specific Ion Parameters. The Journal of Physical Chemistry B 2009, 113 (40), 13279–13290. [PubMed: 19757835]
20. Izadi S; Anandakrishnan R; Onufriev AV, Building Water Models: A Different Approach. The Journal of Physical Chemistry Letters 2014, 5 (21), 3863–3871. [PubMed: 25400877]
21. Loncharich RJ; Brooks BR; Pastor RW, Langevin dynamics of peptides: the frictional dependence of isomerization rates of N-acetylalanyl-N'-methylamide. Biopolymers 1992, 32 (5), 523–35. [PubMed: 1515543]
22. Hermans J; Berendsen HJC; Van Gunsteren WF; Postma JPM, A consistent empirical potential for water–protein interactions. Biopolymers 1984, 23 (8), 1513–1518.
23. Ryckaert J-P; Ciccotti G; Berendsen HJC, Numerical integration of the cartesian equations of motion of a system with constraints: molecular dynamics of n-alkanes. J. Comput. Phys. 1977, 23 (3), 327–341.
24. Hopkins CW; Le Grand S; Walker RC; Roitberg AE, Long-Time-Step Molecular Dynamics through Hydrogen Mass Repartitioning. Journal of Chemical Theory and Computation 2015, 11 (4), 1864–1874. [PubMed: 26574392]
25. Grubbs RH; Miller SJ; Fu GC, Ring-Closing Metathesis and Related Processes in Organic Synthesis. Acc. Chem. Res. 1995, 28 (11), 446–452.
26. Sorensen AM; Nielsen KE; Vogg B; Jacobsen JP; Nielsen P, Synthesis and NMR-studies of dinucleotides with conformationally restricted cyclic phosphotriester linkages. Tetrahedron 2001, 57 (51), 10191–10201.
27. Borsting P; Freitag M; Nielsen P, Dinucleotides containing two allyl groups by combinations of allyl phosphotriesters, 5-allyl-, 2'-O-allyl- and 2'-arabino-O-allyl uridine derivatives as substrates for ring-closing metathesis. Tetrahedron 2004, 60 (48), 10955–10966.
28. Borsting P; Nielsen KE; Nielsen P, Stabilization of a nucleic acid three-way junction by an oligonucleotide containing a single 2'-C to 3'-O-phosphate butylene linkage prepared by a tandem RCM-hydrogenation method. Org. Biomol. Chem. 2005, 3 (11), 2183–2190. [PubMed: 15917908]
29. Borsting P; Christensen MS; Steffansen SI; Nielsen P, Synthesis of dinucleotides with 2'-C to phosphate connections by ring-closing metathesis. Tetrahedron 2006, 62 (6), 1139–1149.
30. Migawa MT; Shen W; Wan WB; Vasquez G; Oestergaard ME; Low A; De Hoyos CL; Gupta R; Murray S; Tanowitz M; Bell M; Nichols JG; Gaus H; Liang XH; Swayze EE; Crooke ST; Seth PP, Site-specific replacement of phosphorothioate with alkyl phosphonate linkages enhances the therapeutic profile of gapmer ASOs by modulating interactions with cellular proteins. Nucleic Acids Res. 2019, 47 (11), 5465–5479. [PubMed: 31034558]
31. Lebedev AV; Frauendorf A; Vyazovkina EV; Engels JW, Determination and prediction of the absolute configuration of dinucleoside alkylphosphonates using conformational analysis and multivariate statistics. Tetrahedron 1993, 49 (5), 1043–1052.
32. Vyazovkina EV; Savchenko EV; Lokhov SG; Engels JW; Wickstrom E; Lebedev AV, Synthesis of specific diastereomers of a DNA methylphosphonate heptamer, d(CpCpApApApCpA), and stability of base pairing with the normal DNA octamer d(TPGPTPTPTPGPGPC). Nucleic Acids Res. 1994, 22 (12), 2404–2409. [PubMed: 8036171]
33. Xu D; Rivas-Bascón N; Padial NM; Knouse KW; Zheng B; Vantourout JC; Schmidt MA; Eastgate MD; Baran PS, Enantiodivergent Formation of C–P Bonds: Synthesis of P-Chiral Phosphines and Methylphosphonate Oligonucleotides. J. Am. Chem. Soc. 2020, 142 (12), 5785–5792. [PubMed: 32109356]

34. Egli M; Portmann S; Usman N, RNA hydration: a detailed look. Biochemistry 1996, 35 (26), 8489–94. [PubMed: 8679609]
35. Tereshko V; Gryaznov S; Egli M, Consequences of Replacing the DNA 3'-Oxygen by an Amino Group: High-Resolution Crystal Structure of a Fully Modified N3'->P5' Phosphoramidate DNA Dodecamer Duplex. J. Am. Chem. Soc. 1998, 120 (2), 269–283.
36. Koshkin AA; Singh SK; Nielsen P; Rajwanshi VK; Kumar R; Meldgaard M; Olsen CE; Wengel J, LNA (locked nucleic acids): synthesis of the adenine, cytosine, guanine, 5-methylcytosine, thymine and uracil bicyclonucleoside monomers, oligomerization, and unprecedented nucleic acid recognition. Tetrahedron 1998, 54 (14), 3607–3630.
37. Obika S; Nanbu D; Hari Y; Andoh J-I; Morio K-I; Doi T; Imanishi T, Stability and structural features of the duplexes containing nucleoside analogs with a fixed N-type conformation, 2'-O,4'-C-methyleneribonucleosides. Tetrahedron Lett. 1998, 39 (30), 5401–5404.
38. Decuypere E; Lepikhina A; Halloy F; Hall J, Increased Affinity of 2′-O-(2-Methoxyethyl)-Modified Oligonucleotides to RNA through Conjugation of Spermine at Cytidines. Helv. Chim. Acta 2019, 102 (12), e1900222.
39. Menzi M; Wild B; Pradère U; Malinowska AL; Brunschweiger A; Lightfoot HL; Hall J, Towards Improved Oligonucleotide Therapeutics Through Faster Target Binding Kinetics. *Chemistry* – A European Journal 2017, 23 (57), 14221–14230.
40. Jensen KK; Ørum H; Nielsen PE; Nordén B, Kinetics for Hybridization of Peptide Nucleic Acids (PNA) with DNA and RNA Studied with the BIAcore Technique. Biochemistry 1997, 36 (16), 5072–5077. [PubMed: 9125529]
41. Kasuya T; Kugimiya A, Role of Computationally Evaluated Target Specificity in the Hepatotoxicity of Gapmer Antisense Oligonucleotides. Nucleic Acid Ther. 2018, 28 (5), 312–317. [PubMed: 30095329]
42. Dieckmann A; Hagedorn PH; Burki Y; Brügmann C; Berrera M; Ebeling M; Singer T; Schuler F, A Sensitive In Vitro Approach to Assess the Hybridization-Dependent Toxic Potential of High Affinity Gapmer Oligonucleotides. Mol. Ther. Nucleic Acids 2018, 10 (Supplement C), 45–54. [PubMed: 29499955]
43. Kamola PJ; Maratou K; Wilson PA; Rush K; Mullaney T; McKevitt T; Evans P; Ridings J; Chowdhury P; Roulois A; Fairchild A; McCawley S; Cartwright K; Gooderham NJ; Gant TW; Moores K; Hughes SA; Edbrooke MR; Clark K; Parry JD, Strategies for In Vivo Screening and Mitigation of Hepatotoxicity Associated with Antisense Drugs. Mol. Ther. Nucleic Acids 2017, 8 (Supplement C), 383–394. [PubMed: 28918038]
44. Burel SA; Hart CE; Cauntay P; Hsiao J; Machemer T; Katz M; Watt A; Bui HH; Younis H; Sabripour M; Freier SM; Hung G; Dan A; Prakash TP; Seth PP; Swayze EE; Bennett CF; Crooke ST; Henry SP, Hepatotoxicity of high affinity gapmer antisense oligonucleotides is mediated by RNase H1 dependent promiscuous reduction of very long pre-mRNA transcripts. Nucleic Acids Res. 2016, 44 (5), 2093–109. [PubMed: 26553810]
45. Shen W; De Hoyos CL; Migawa MT; Vickers TA; Sun H; Low A; Bell TA 3rd; Rahdar M; Mukhopadhyay S; Hart CE; Bell M; Riney S; Murray SF; Greenlee S; Crooke RM; Liang XH; Seth PP; Crooke ST, Chemical modification of PS-ASO therapeutics reduces cellular protein-binding and improves the therapeutic index. Nat. Biotechnol. 2019, 37 (6), 640–650. [PubMed: 31036929]

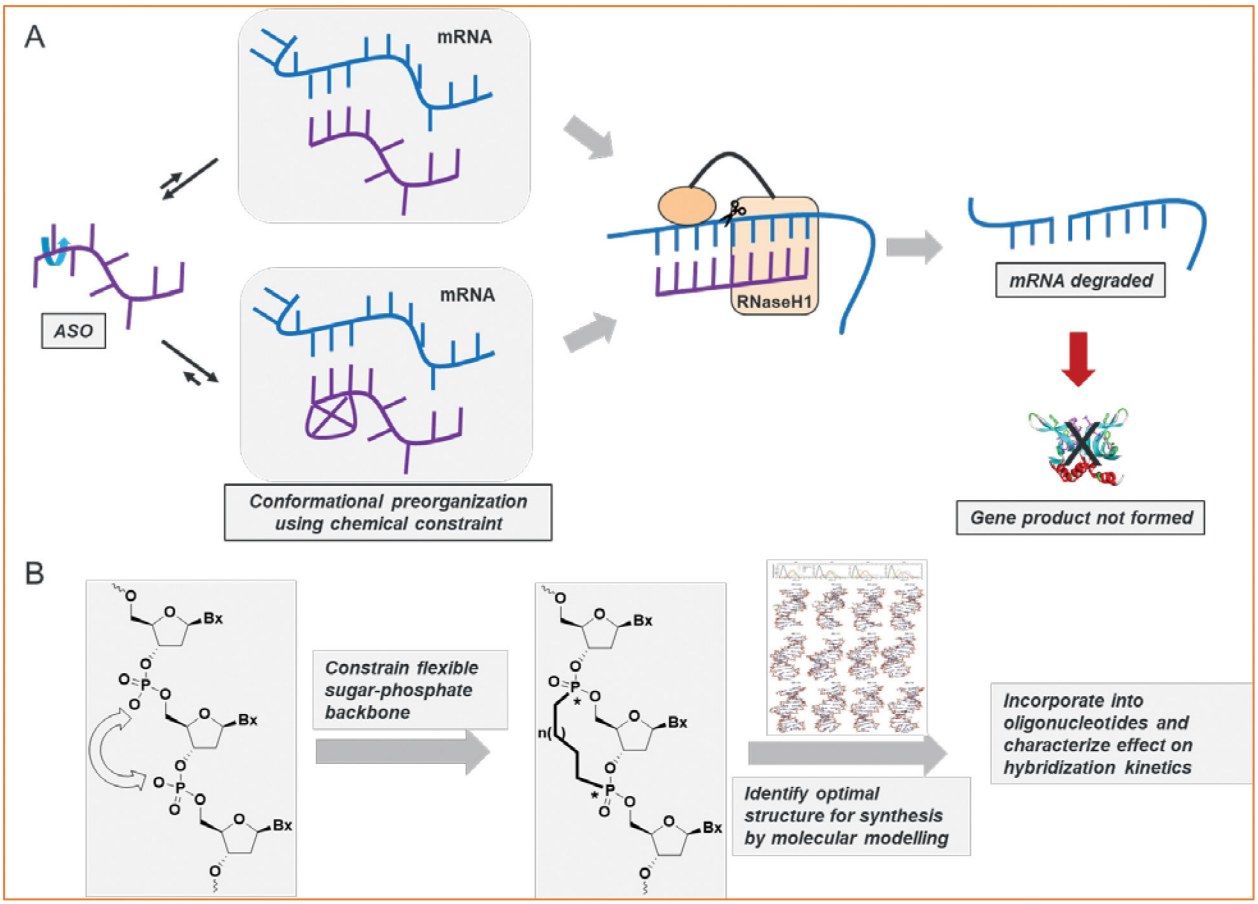

Figure 1.

(A) Appropriate conformational constraint can pre-organize a therapeutic oligonucleotide for more efficient hybridization with its targeted mRNA. (B) Design of phosphonate ester backbone constrained nucleic acid analogs

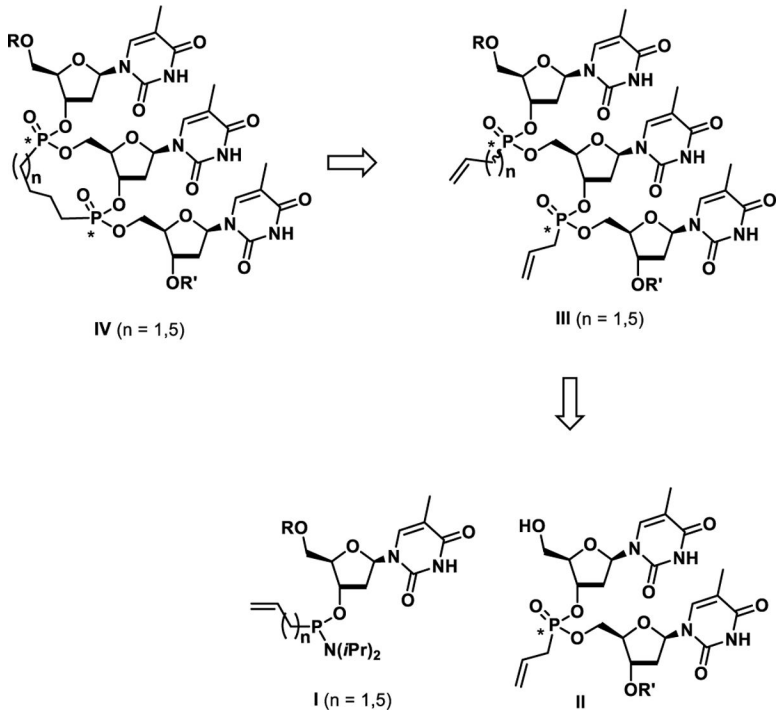

Figure 2 –.
Retrosynthesis of backbone constrained nucleic acids

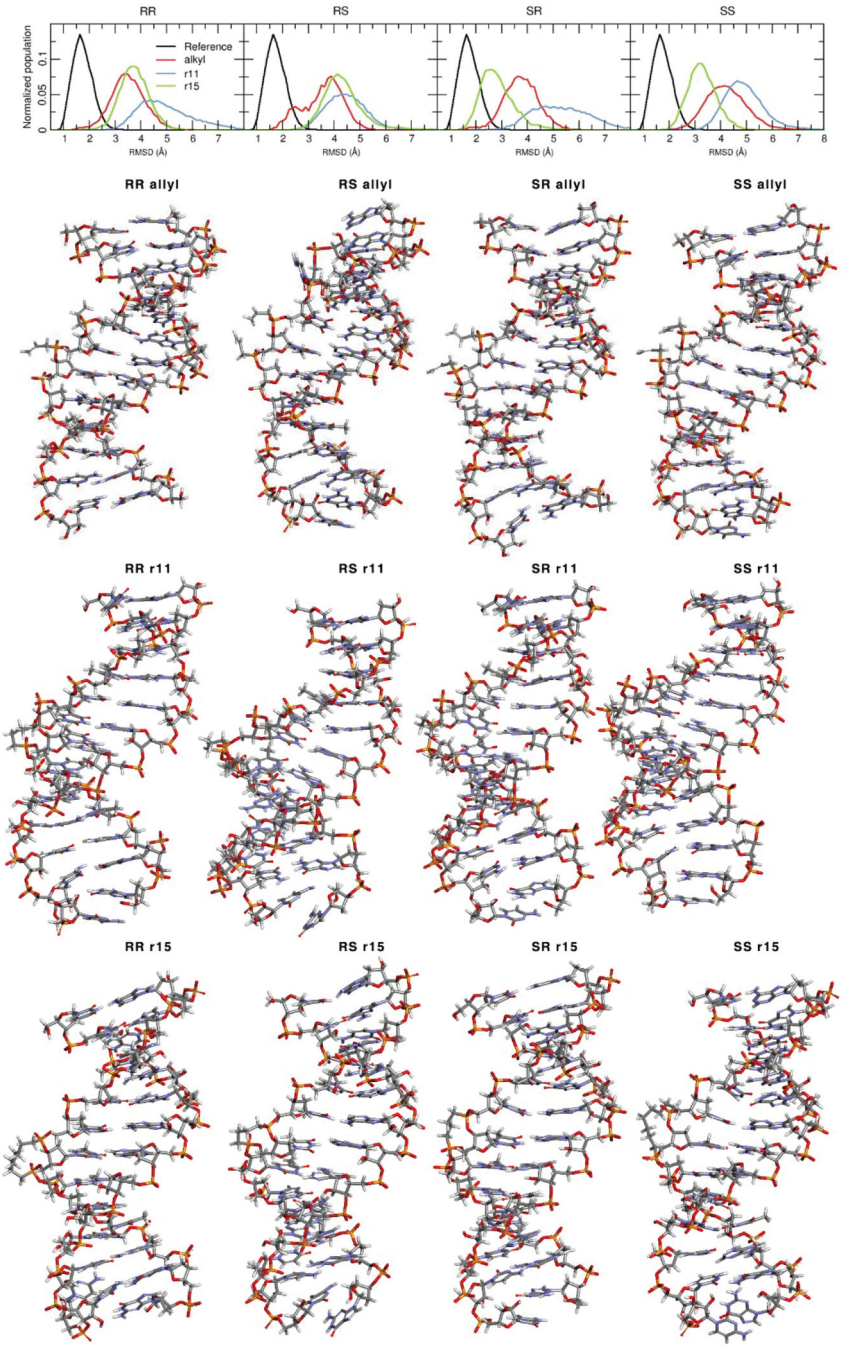

Figure 3.

Normalized distribution of the RMSD values for each of the modeled systems. The RMSD calculated values are only considering the inner base-pairs and using the first frame as reference. Bottom molecular images show the representative structure of the most populated cluster for each simulation. All sampled frames from the MD trajectory (each ps) were considered for the clustering analysis.

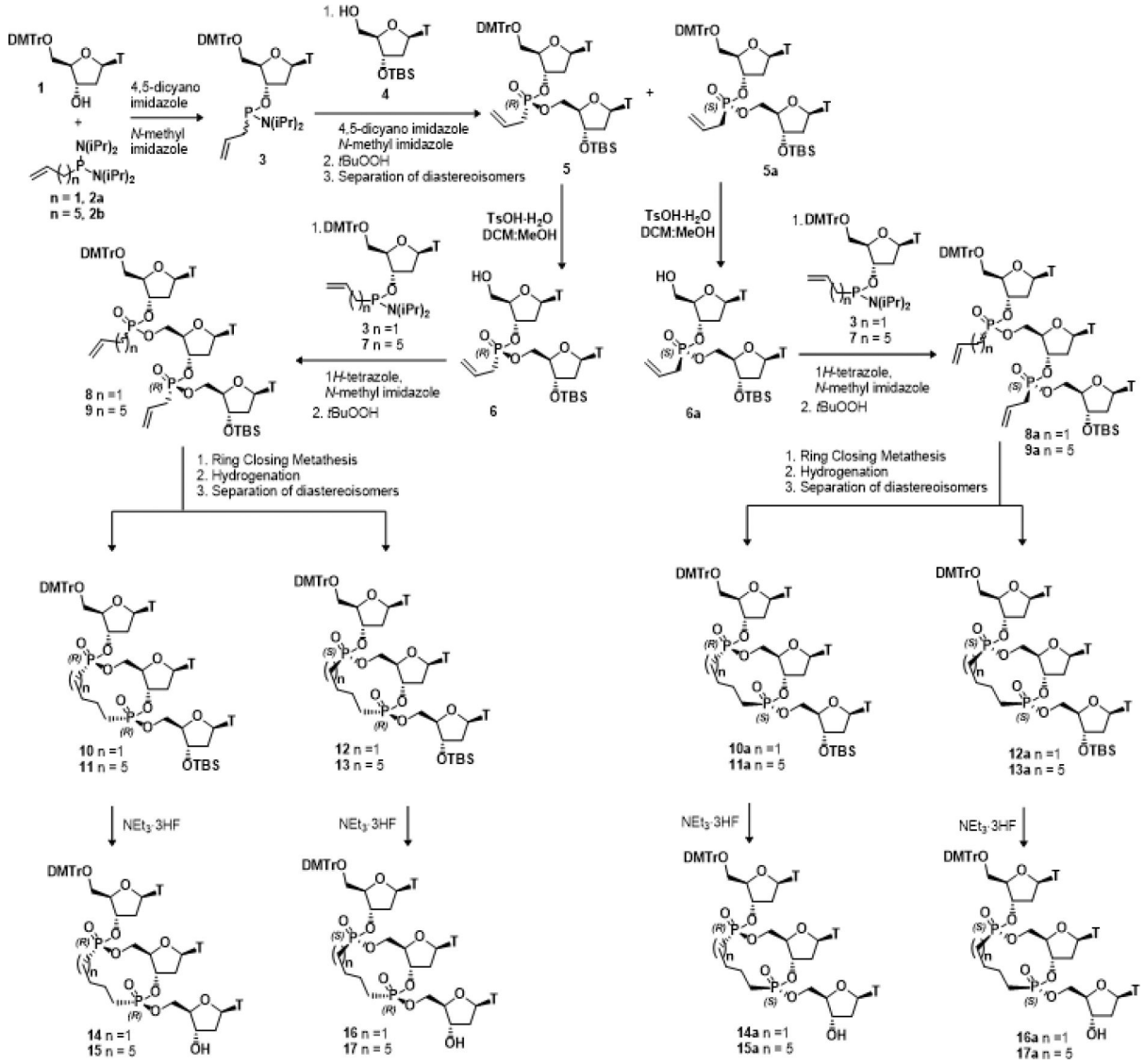

Scheme 1.

Synthesis of 11- and 15-membered P-macrocyclic 2’-deoxythymidine trimers

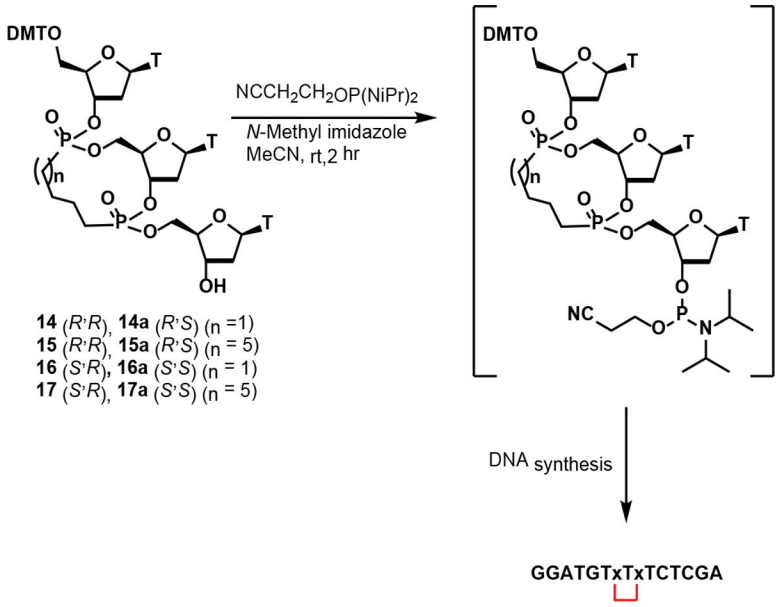

Scheme 2.

Incorporation of backbone-constrained nucleic acids into oligonucleotides

Table 1.

Duplex stabilizing properties and hybridization kinetics versus complementary RNA of phosphate backbone constrained macrocyclic nucleic acid analogs. Binding of oligonucleotides to complement RNA was performed on a Biacore X100 surface plasmon resonance (SPE) instrument. 100 units of complementary RNA was immobilized on a SA chip by injecting a 20 nM solution of 5'-Biotin-labeled RNA (5'-Biotin-UCGAGAAACAUCC-3') in HPS-EP buffer (10 mM HEPES, pH 7.4, 150 mM NaCl, 3 mM EDTA, 0.0005% Surfactant P20). Binding was evaluated by injecting increasing concentration of oligonucleotides (6.75nM to 100 nM, 2-fold dilution) in HPB-EP buffer at 25°C onto RNA-immobilized SA chip. Kinetic and equilibrium binding analysis was performed using Biacore X100 Evaluation Software applying 1:1 binding fit.

ON	Sequence	macrocycle		Tm (°C)	ΔTm (°C)		K_D nM	K_{on} $M^{-1}S^{-1}$	K_{off} S^{-1}
		size	P config.		DNA parent	open-allyl			
1	**GGATGTTTCTCGA**	PO DNA	--	49.5	--	--	0.26	4.44×10^5	11.3×10^{-5}
2	**GGATGTxTxTCTCGA**	Bis-allyl	**S,R**	42.8	−6.7	--	1.35	6.04×10^5	81.5×10^{-5}
3	**GGATGTxTxTCTCGA**	Bis-allyl	**S,S**	38.1	−11.4	--	13.8	1.96×10^5	271×10^{-5}
4	**GGATGTxTxTCTCGA**	Bis-allyl	**R,S**	42.4	−7.1	--	1.19	6.60×10^5	78.8×10^{-5}
5	**GGATGTxTxTCTCGA**	Bis-allyl	**R,R**	46.9	−2.6	--	0.39	5.17×10^5	20.3×10^{-5}
6	**GGATGTxTxTCTCGA**	11	**S,R**	34.4	−15.1	−8.4	nd	nd	nd
7	**GGATGTxTxTCTCGA**	11	**S,S**	31.7	−17.8	−6.4	nd	nd	nd
8	**GGATGTxTxTCTCGA**	11	**R,S**	33.7	−15.8	−8.7	nd	nd	nd
9	**GGATGTxTxTCTCGA**	11	**R,R**	30.3	−19.2	−16.6	nd	nd	nd
10	**GGATGTxTxTCTCGA**	15	**S,R**	48.4	−1.1	+5.6	0.34	5.36×10^5	18.1×10^{-5}
11	**GGATGTxTxTCTCGA**	15	**S,S**	41.1	−8.4	+3.0	2.18	18.9×10^5	412×10^{-5}
12	**GGATGTxTxTCTCGA**	15	**R,S**	46.4	−3.1	+4.0	0.16	7.12×10^5	11.4×10^{-5}
13	**GGATGTxTxTCTCGA**	15	**R,R**	42.4	−7.1	−4.5	0.70	6.66×10^5	88.0×10^{-5}
14	**GGATGTTTCTCGA**	1 LNA	--	58.2		--	< 0.06	8.10×10^5	$< 5 \times 10^{-5}$
15	**GGATGTTTCTCGA**	1 LNA	--	58.1		--	< 0.07	7.74×10^5	$< 5 \times 10^{-5}$
16	**GGATGTTTCTCGA**	1 LNA	--	58.6		--	< 0.09	5.11×10^5	$< 5 \times 10^{-5}$
17	**GGATGTTTCTCGA**	3 LNA	--	68.8		--	< 0.06	8.88×10^5	$< 5 \times 10^{-5}$